

Effect of dipole polarizability on positron binding by strongly polar molecules

G F Gribakin and A R Swann¹

Centre for Theoretical Atomic, Molecular and Optical Physics, School of Mathematics and Physics,
Queen's University Belfast, Belfast BT7 1NN, UK

E-mail: g.gribakin@qub.ac.uk and aswann02@qub.ac.uk

Received 23 April 2015, revised 24 August 2015

Accepted for publication 26 August 2015

Published 23 September 2015



CrossMark

Abstract

A model for positron binding to polar molecules is considered by combining the dipole potential outside the molecule with a strongly repulsive core of a given radius. Using existing experimental data on binding energies leads to unphysically small core radii for all of the molecules studied. This suggests that electron–positron correlations neglected in the simple model play a large role in determining the binding energy. We account for these by including the polarization potential via perturbation theory and non-perturbatively. The perturbative model makes reliable predictions of binding energies for a range of polar organic molecules and hydrogen cyanide. The model also agrees with the linear dependence of the binding energies on the polarizability inferred from the experimental data (Danielson *et al* 2009 *J. Phys. B: At. Mol. Opt. Phys.* **42** 235203). The effective core radii, however, remain unphysically small for most molecules. Treating molecular polarization non-perturbatively leads to physically meaningful core radii for all of the molecules studied and enables even more accurate predictions of binding energies to be made for nearly all of the molecules considered.

Keywords: positron, polar molecule, binding energy, polarizability, dipole, polarization

(Some figures may appear in colour only in the online journal)

1. Introduction

Positrons are a useful tool in many areas of science, such as condensed matter physics, surface science and medicine (see, e.g., [1, 2]). Despite this, there is still much about their interactions with ordinary matter that remains to be explored theoretically. In particular, the binding of positrons to matter has been a difficult subject to research [3]. On the part of theory, this is due to the strong electron–positron correlations which determine the binding energy and, in many cases, ensure the very existence of bound states. On the experimental side, positron binding to atoms has not been verified experimentally, largely due to the difficulty in obtaining the relevant species in the gas phase. On the other hand, for polyatomic molecules a wealth of information is now available thanks to the special role that vibrational Feshbach resonances play in positron–molecule annihilation [4].

Before a positron annihilates with an electron in a molecule, it usually forms a quasibound state with the molecule by transferring its excess energy into vibrations of a single mode with near-resonant energy. This leads to pronounced resonances observed in the positron-energy dependence of the annihilation rate [4, 5]. Using the relation

$$\epsilon_\nu = \omega_\nu - \epsilon_b \quad (1)$$

where ϵ_ν is the energy of the resonance due to vibrational mode ν with energy ω_ν , experimentalists have now been able to measure values of the positron binding energy ϵ_b for over sixty molecules [6, 7]. These measurements led to the construction of a phenomenological parametric fit of ϵ_b in terms of the dipole polarizability α and permanent dipole moment μ of the molecule:

$$\epsilon_b = 12.4(\alpha + 1.6\mu - 5.6), \quad (2)$$

where ϵ_b is in milli-electron volts, α is in cubic angstroms and μ is in debyes (D) [8]. An interesting feature of (2) is that the dependences of ϵ_b on μ and α are both linear. Although a

¹ Author to whom any correspondence should be addressed.

general increase of ϵ_b with μ and α is to be expected (since both contribute to the positron–molecule attraction), there is no obvious reason why the dependences should be linear. In fact, measurements for some molecules with large dipole moments, such as acetone and acetonitrile, yielded binding energies more than double the values predicted by equation (2) [6].

Despite the wealth of experimental data on positron–molecule binding energies, theoretical developments are somewhat behind. There are few calculations of positron binding to nonpolar or weakly polar molecules. The zero-range potential model [9, 10] captured the qualitative features of the binding for alkanes and correctly predicted the emergence of the second bound state [9]. There were also predictions of positron binding to the hydrogen molecule in the excited $A\ ^3\Sigma_u$ state [11], and configuration interaction (CI) calculations for carbon-containing triatomics (CO_2 , CS_2 , CSe_2 and weakly polar COS , COSe and CSSe) [12, 13]. The latter papers reported binding by the two heaviest species in the vibrational ground state, by CS_2 in the lowest vibrationally excited states, and by other molecules at higher vibrational excitations or upon bond deformations. In contrast, there is a large number of quantum chemistry calculations of positron binding with strongly polar polyatomic molecules with dipole moments $\gtrsim 3$ D. For such molecules binding is achieved even at the lowest, static-field (e.g., Hartree–Fock (HF)) level of theory. The static-field binding energies, however, are usually quite small, and the effect of correlations (e.g., polarization of the molecule by the positron) increases the binding energy dramatically (see, e.g., [14–18]). Recent configuration interaction calculations for nitriles, acetaldehyde, and acetone [19–21] in fact give binding energies within 25%–50% of the experiment, which is quite good, given the complexity of the system.

The purpose of this article is to present a simple model for positron binding to polar molecules. For many molecules of interest the dipole moment is dominated by a single bond (e.g., CN or CO), located at one end of the molecule, with the negative charge on the terminal atom. Given the positron repulsion from the atomic nuclei, we model the molecular potential as a point dipole surrounded by an impenetrable sphere. Of course, the true size of the molecular dipole is finite, of the order of interatomic distances. However, for weakly bound positron states, the wave function of the positron is very diffuse. Its spatial extent is much greater than the physical size of the dipole, which justifies the applicability of the point-dipole model to weakly bound positron states. This is illustrated by figure 1, which shows the density for the positron bound in the dipole field of the acetonitrile molecule (CH_3CN). The figure also shows that the positron is localized in the negative-energy well of the dipole potential and is largely ‘unaware’ of the true geometry of the molecule. This justifies the hard-sphere model for the short-range positron repulsion. Quantum chemistry calculations of the positron density in polar molecules support the picture of a diffuse positronic cloud localized off the negatively charged end of the molecular dipole [14, 17, 19, 20].

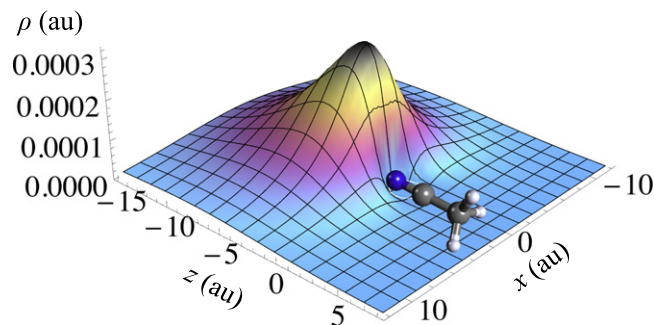


Figure 1. The density of the positron bound in the field of a point dipole with the dipole moment $\mu = 3.93$ D of the acetonitrile molecule and repulsive core of the radius $r_0 = 1.175$ au, with the binding energy of $\epsilon_b = 27$ meV.

Note that a recent paper [22] combined a hard-sphere repulsive core with the polarization potential to model positron binding to atoms and nonpolar molecules. While the two models bear some similarity, the physics of positron binding to neutral atoms and nonpolar species is very different from that of binding to strongly polar molecules explored in this work. In the former case, for atoms the positron does form a spherical cloud, but for molecules the shape of the positron wave function largely repeats that of the molecule [10], and the spherical repulsive core approximation is hard to justify. In contrast, for bound states with polar species, the positron resides in the dipole-generated well to one side of the molecule (see figure 1), and the repulsive core model looks more appropriate.

The main features of binding by the dipole potential are outlined in section 2. Applying the model to polar molecules for which the positron binding energies are known from experiment (section 3) shows that electron–positron correlations have a large effect on binding. We include these in the form of the polarization potential, first via perturbation theory (section 4) and then non-perturbatively (section 5). While this model may appear to be rather crude, it captures the main physical aspects of the problem. Owing to its simplicity, it provides a deeper understanding of some of the key features that have been observed in experiment, including the empirical scaling (2). The usefulness of such models as a means of obtaining an *explanation*, and complementary to heavy numerical computations, was argued well by Ostrovsky, who introduced the notion of complementarity between calculation and explanation [23, 24].

2. Theory

We model the molecule as an impenetrable sphere of radius r_0 , with a point dipole of dipole moment μ fixed at its centre (the origin). The positron experiences point-dipole potential in the region outside the sphere. Using spherical polar coordinates (r, θ, ϕ) and choosing the polar (z -) axis along μ , we

have

$$V_d(\mathbf{r}) = \begin{cases} \infty & \text{for } r \leq r_0, \\ \mu r^{-2} \cos \theta & \text{for } r > r_0, \end{cases} \quad (3)$$

where θ is the polar angle, and we work in atomic units (au).

Although (3) is a non-central potential, the Schrödinger equation,

$$\left[-\frac{1}{2}\nabla^2 + V_d(\mathbf{r}) \right] \psi(\mathbf{r}) = E\psi(\mathbf{r}), \quad (4)$$

for the positron wave function $\psi(\mathbf{r})$ and energy E can be solved in the region $r > r_0$ using separation of variables. Inserting the ansatz $\psi(\mathbf{r}) = R(r)\Phi(\theta, \phi)$ into (4) yields separate radial and angular equations:

$$\frac{1}{r^2} \frac{d}{dr} \left(r^2 \frac{dR}{dr} \right) + \left(2E - \frac{\lambda}{r^2} \right) R = 0, \quad (5a)$$

$$\frac{1}{\sin \theta} \frac{\partial}{\partial \theta} \left(\sin \theta \frac{\partial \Phi}{\partial \theta} \right) + \frac{1}{\sin^2 \theta} \frac{\partial^2 \Phi}{\partial \phi^2} + (\lambda - 2\mu \cos \theta) \Phi = 0, \quad (5b)$$

where λ is a separation constant. If $\mu = 0$ then (5b) becomes $(\hat{L}^2 - \lambda)\Phi = 0$, where \hat{L}^2 is the squared angular momentum operator. This is just the eigenvalue equation for the \hat{L}^2 operator; the possible values of λ are $l(l+1)$, where l (the azimuthal quantum number) is a non-negative integer, and the eigenfunctions are the spherical harmonics $Y_{lm}(\theta, \phi)$, where m (the magnetic quantum number) is the eigenvalue of \hat{L}_z , and m is an integer, $|m| \leq l$.

For $\mu \neq 0$, l is no longer a good quantum number since \hat{L}^2 does not commute with the Hamiltonian. However, \hat{L}_z does commute with the Hamiltonian, and thus m is still a good quantum number. We must solve the angular equation (5b) to find the new values of λ . With this information we will be able to solve the radial equation and use it to investigate the dependence of the binding energy $\epsilon_b = |E|$ on μ and r_0 .

2.1. Angular equation

Since m is a good quantum number, there will be a distinct set of eigenfunctions $\Phi_m(\theta, \phi)$ of the angular equation (5b) for each value of m . We expand the unknown functions in the basis of spherical harmonics, i.e.

$$\Phi_m(\theta, \phi) = \sum_{l'=|m|}^{\infty} C_{l'm} Y_{l'm}(\theta, \phi) \quad (m = 0, \pm 1, \pm 2, \dots), \quad (6)$$

where the $C_{l'm}$ are unknown numbers. Substituting this expression into (5b), multiplying across by $Y_{lm}^*(\theta, \phi)$, where l is a non-negative integer such that $l \geq |m|$, integrating over ϕ and θ and using properties of spherical harmonics (see, e.g., [25]) yields

$$\sum_{l'=|m|}^{\infty} B_{l'l'm} C_{l'm} = \lambda_m C_{lm}, \quad (7)$$

where

$$B_{l'l'm} = l(l+1)\delta_{l'l'} + 2\mu(-1)^m \times \sqrt{(2l+1)(2l'+1)} \begin{pmatrix} 1 & l & l' \\ 0 & 0 & 0 \end{pmatrix} \begin{pmatrix} 1 & l & l' \\ 0 & -m & m \end{pmatrix}, \quad (8)$$

and the arrays in parentheses are $3j$ symbols. The eigenvalue λ has been renamed λ_m since it will have different sets of values depending on m . Equations (7) are a set of matrix eigenvalue equations for the semi-infinite, symmetric, tridiagonal matrix $B_{l'l'm}$, whose rows and columns are enumerated by l and l' , respectively. Each of these matrices has a countably infinite set of eigenvalues, so we rename λ_m as λ_{ms} , where $s = 1, 2, 3, \dots$ enumerates the different eigenvalues for each m , and the eigenvalues are arranged so that $\lambda_{m1} < \lambda_{m2} < \lambda_{m3} < \dots$. Symmetry properties of the $3j$ symbols can easily be used to show that $B_{l'l',-m} = B_{l'l'm}$, and so (7) need only be solved for $m \geq 0$.

We seek bound states of the positron. From the form of the radial equation (5a) it can be shown that for $\lambda_{ms} < -\frac{1}{4}$ there will be an infinite number of bound states, while for $\lambda_{ms} > -\frac{1}{4}$ there will be none [26] (see section 2.2). Given a certain value of μ and of m , by truncating the infinite matrix $B_{l'l'm}$ to a finite size (where the final row and column are denoted by $l = l' = l_{\max}$), we can find numerical approximations for the first $l_{\max} - |m| + 1$ values of λ_{ms} . Table 1 and figure 2 show how λ_{m1} , λ_{m2} and λ_{m3} vary with μ for $m = 0$ and $m = \pm 1$. Values of l_{\max} shown in the last column of table 1 are chosen so that the eigenvalues are correct to at least six decimal places.

Considering the eigenvalues λ_{ms} as functions of μ , for each combination of m and s there is a critical dipole moment μ_{crit} for which $\lambda_{ms} = -\frac{1}{4}$. Some of these critical dipole moments are shown in table 2; they agree with the values obtained by Fermi and Teller [27] and Crawford [28]. The condition $\mu > \mu_{\text{crit}}$ guarantees binding by either a point-like or finite dipole. The smallest critical dipole is $\mu_{\text{crit}} = 1.625$ D for $m = 0, s = 1$. Since typical molecules have dipole moments not exceeding 11 D, i.e., up to 4.3 au, the only possible bound states are those corresponding to $m = 0, s = 1$ and $m = \pm 1, s = 1$. The critical value of μ needed to sustain any other bound state is simply too high.

It must be mentioned that the above considerations apply to binding by the static dipole, i.e., assuming that the molecules cannot rotate. When rotations are included, the values of μ_{crit} required for the dipole binding to occur are 10%–30% greater [29]. This gap depends on the moment of inertia of the molecule and increases with the molecular angular momentum, being smallest for large, slowly rotating molecules. Another consideration important for *ab initio* quantum-chemistry calculations of binding is that for the values of μ only slightly exceeding μ_{crit} , the binding energy is very sensitive to the actual value of the dipole moment (see figure 3 in section 2.3). The actual value of the dipole moment depends on the approximation used (e.g., HF), and can be a significant source of error [30]. However, both the effect of molecular rotations and the sensitivity to the value of μ are offset by the

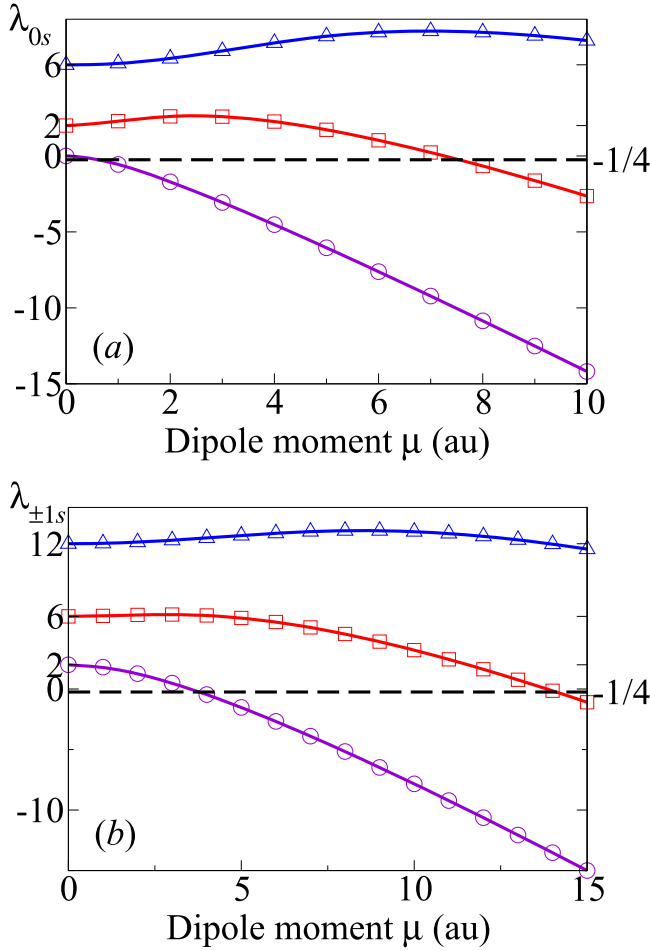


Figure 2. Dependence of the eigenvalues λ_{m1} (purple circles), λ_{m2} (red squares) and λ_{m3} (blue triangles) for (a) $m = 0$ and (b) $m = \pm 1$, on the dipole moment μ . Intersections with the dashed lines ($\lambda = -1/4$) give critical dipole moments μ_{crit} .

Table 2. Critical dipole moments required for various bound states of the positron, along with the values of l_{max} required for stability to 10^{-6} au.

$ m $	s	$\mu_{\text{crit}}(\text{au})$	$\mu_{\text{crit}}(\text{D})$	l_{max}
0	1	0.639 315	1.625	4
0	2	7.546 956	19.182	10
1	1	3.791 968	9.634	8
1	2	14.112 115	35.869	12
2	1	9.529 027	24.220	10

large contribution of electron–positron correlations to the positron binding (see sections 4 and 5).

2.2. Radial equation

Under the substitution

$$R(r) = \frac{Z(kr)}{\sqrt{kr}}, \quad (9)$$

where $k = \sqrt{2E}$, the radial equation (5a) yields the following differential equation for $Z(kr)$:

$$(kr)^2 \frac{d^2 Z}{d(kr)^2} + kr \frac{dZ}{d(kr)} + \left[(kr)^2 - \left(\lambda_{ms} + \frac{1}{4} \right) \right] = 0. \quad (10)$$

This is just Bessel’s differential equation. Since for bound states we have $E < 0$, i.e., $E = -|E|$, it is best to express the general solution in terms of modified Bessel functions:

$$Z_{ms}(kr) = A_{ms} K_{i\beta_{ms}}(\kappa r) + B_{ms} I_{i\beta_{ms}}(\kappa r), \quad (11)$$

where the subscripts m and s have been added to Z because there is a distinct function for each combination of m and s , A_{ms} and B_{ms} are arbitrary constants, $\kappa = \sqrt{2|E|}$, and

$$\beta_{ms} = \left| \lambda_{ms} + \frac{1}{4} \right|^{1/2}, \quad (12)$$

and $\lambda_{ms} < -\frac{1}{4}$ is assumed. Equation (9) then gives

$$R_{ms}(r) = A_{ms} \frac{K_{i\beta_{ms}}(\kappa r)}{\sqrt{\kappa r}} + B_{ms} \frac{I_{i\beta_{ms}}(\kappa r)}{\sqrt{\kappa r}}. \quad (13)$$

For the bound-state wave function to be normalizable we must require $R_{ms}(r) \rightarrow 0$ as $r \rightarrow \infty$. It can be seen from the asymptotic forms of the modified Bessel functions (see, e.g., [31]) that $I_\nu(x)/\sqrt{x} \rightarrow \infty$ as $x \rightarrow \infty$, while $K_\nu(x)/\sqrt{x} \rightarrow 0$ as $x \rightarrow \infty$, assuming that x is real. We therefore require $B_{ms} = 0$ for every m and s , and so

$$R_{ms}(r) = A_{ms} \frac{K_{i\beta_{ms}}(\kappa r)}{\sqrt{\kappa r}}, \quad (14)$$

with A_{ms} a constant of normalization.

Since κr and β_{ms} are real and positive, the function $K_{i\beta_{ms}}(\kappa r)$ (also known as the Macdonald function) is also real, which can be seen, e.g., from the integral representation [32]

$$K_{i\beta_{ms}}(\kappa r) = \int_0^\infty \exp(-\kappa r \cosh t) \cos(\beta_{ms} t) dt, \quad (15)$$

and thus $R_{ms}(r)$ is real (for a real A_{ms}). The function $R_{ms}(r)$ has infinitely many positive roots, with an accumulation point at $r = 0$.

The second boundary condition to be applied to $R_{ms}(r)$ is due to the impenetrable sphere at $r = r_0$, which means that we must have $R_{ms}(r_0) = 0$, i.e.

$$\frac{K_{i\beta_{ms}}(\kappa r_0)}{\sqrt{\kappa r_0}} = 0. \quad (16)$$

The positive roots of the function $K_{i\beta_{ms}}(z)$ are therefore the allowed values of κr_0 . Since these roots form an infinite, discrete set, we shall name them ζ_{msn} , where $n = 1, 2, 3, \dots$, and $\zeta_{ms1} > \zeta_{ms2} > \zeta_{ms3} > \dots$. These roots can be found numerically. For any particular molecule, r_0 is a constant, and so the permissible values of κ (which we now rename κ_{msn} , and likewise with E) are $\kappa_{msn} = \zeta_{msn}/r_0$, i.e.

$$E_{msn} = -\frac{\kappa_{msn}^2}{2} = -\frac{1}{2} \left(\frac{\zeta_{msn}}{r_0} \right)^2. \quad (17)$$

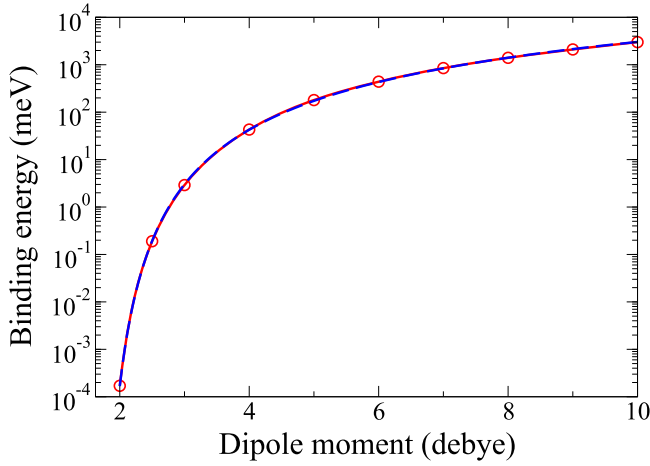


Figure 3. Dependence of the ground-state binding energy ϵ_b on μ for $r_0 = 1$. Solid red line with circles shows the numerical results, and the blue dashed line is the fit (23) with $A = 65998.7$ meV, $B = 12.2705$ D $^{1/2}$, and $C = 0.400612$ D $^{-1/2}$. Note that the two curves are indistinguishable on the scale of the graph.

2.3. Dependence of binding energy on r_0 and μ

For a given value of the dipole moment, the largest negative value of λ_{ms} is for $m = 0$, $s = 1$, with the critical dipole moment $\mu_{\text{crit}} = 0.6393$ au = 1.625 D [27, 28]. The corresponding ground-state binding energy is

$$\epsilon_b = \frac{1}{2} \left(\frac{\zeta_{011}}{r_0} \right)^2, \quad (18)$$

where ζ_{011} is the largest root of $K_{i\beta_{01}}(z)$, whose index β_{01} is determined by the eigenvalue λ_{01} of the angular equation, see (12). The dependence of the binding energy (18) on r_0 is simple. Figure 3 shows the dependence of ϵ_b on the magnitude of the dipole moment μ for the fixed repulsive core radius $r_0 = 1$ au (i.e., $\epsilon_b = \frac{1}{2}\zeta_{011}^2$).

For $\mu \rightarrow \mu_{\text{crit}}$, the binding energy rapidly tends to zero. This limit corresponds to $\lambda_{01} \rightarrow -\frac{1}{4}$ and $\beta_{01} \rightarrow 0$. In the limit of small β , the roots z_n of the Macdonald function $K_{i\beta}(z)$ have the following asymptotic behaviour [33]:

$$\ln z_n \simeq -\frac{n\pi}{\beta} + \ln 2 - \gamma \quad (n = 1, 2, \dots), \quad (19)$$

where $\gamma \approx 0.577$ is Euler's constant. The largest root that we are interested in ($n = 1$) is then given by

$$\zeta_{011} \simeq 2e^{-\gamma} \exp\left(-\frac{\pi}{\beta_{01}}\right). \quad (20)$$

For dipole moments close to the critical value, we have from equation (12),

$$\beta_{01} \simeq \left[-\frac{d\lambda_{01}}{d\mu} \Big|_{\mu=\mu_{\text{crit}}} (\mu - \mu_{\text{crit}}) \right]^{1/2}. \quad (21)$$

Combining equations (18), (20) and (21), gives

$$\epsilon_b = A \exp\left[-B(\mu - \mu_{\text{crit}})^{-1/2}\right], \quad (22)$$

Table 3. Values of r_0 obtained for a selection of molecules by fitting known binding energies from [7, 36, 38] to equation (18).

Molecule	μ (D)	ϵ_b (meV)	r_0 (au)
Aldehydes			
Acetaldehyde (C ₂ H ₄ O)	2.75	88	1.03×10^{-1}
Propanal (C ₃ H ₆ O)	2.52	118	4.28×10^{-2}
Butanal (C ₄ H ₈ O)	2.72	142	7.44×10^{-2}
Ketones			
Acetone (C ₃ H ₆ O)	2.88	174	1.00×10^{-1}
2-butanone (C ₄ H ₈ O)	2.78	194	7.45×10^{-2}
Cyclopentanone (C ₅ H ₈ O)	3.30	230	1.90×10^{-1}
Formates			
Methyl formate (C ₂ H ₄ O ₂)	1.77	65	4.04×10^{-6}
Ethyl formate (C ₃ H ₆ O ₂)	1.98	103	9.76×10^{-3}
Propyl formate (C ₄ H ₈ O ₂)	1.89	126	1.77×10^{-4}
Acetates			
Methyl acetate (C ₃ H ₆ O ₂)	1.72	122	7.38×10^{-8}
Ethyl acetate (C ₄ H ₈ O ₂)	1.78	160	4.32×10^{-6}
Nitriles			
Acetonitrile (C ₂ H ₃ N)	3.93	180	4.54×10^{-1}
Propionitrile (C ₃ H ₅ N)	4.05	245	4.37×10^{-1}
2-methylpropionitrile (C ₄ H ₇ N)	4.29	274	5.04×10^{-1}
Methyl halides			
Methyl fluoride (CH ₃ F)	1.86	0.3	1.72×10^{-3}
Methyl chloride (CH ₃ Cl)	1.90	25	1.68×10^{-5}
Methyl bromide (CH ₃ Br)	1.82	40	1.67×10^{-6}

where A and B are constants (see also [34, 35], from which a similar result can be derived). Motivated by this scaling, we constructed an approximate analytical expression for the binding energy as a function of μ in the following form:

$$\epsilon_b = A \exp\left[-B(\mu - \mu_{\text{crit}})^{-1/2} + C(\mu - \mu_{\text{crit}})^{1/2}\right]. \quad (23)$$

Here the second term in the exponent represents a correction to the leading term (22). It accounts for the next order corrections in both (20) and (21), and extends the applicability of (23) way beyond the range of near-critical μ . Regarding the constants A , B and C as fitting parameters, an excellent fit of the numerical data over the whole range covered by figure 3 is obtained using $A = 65998.7$ meV, $B = 12.2705$ D $^{1/2}$ and $C = 0.400612$ D $^{-1/2}$, and the dipole moment μ in debye (D).

3. Positron binding by the dipole potential

Using experimental data on positron binding energies from [7, 36] and dipole moments from [37], we fitted the energies to equation (18) by adjusting the values of r_0 for fourteen polar organic molecules and three polar inorganic molecules¹. No direct experimental binding energy is available for methyl fluoride (CH₃F), and the value obtained by fitting theoretical annihilation rate to experiment has been used instead [38]. If

¹ The methyl halide molecules are quite distinct from the other molecules studied. Each of them contains a different halogen atom. It is this, rather than the size of the molecule, that affects their dipole polarizability.

Table 1. Values of λ_{ms} for $m = 0, \pm 1, s = 1, 2, 3$ across a range of values of the dipole moment μ . The values of l_{\max} needed for stability to six decimal places are also shown.

$ m $	μ (au)	λ_{m1}	λ_{m2}	λ_{m3}	l_{\max}
0	0	0.000 000	2.000 000	6.000 000	2
0	2	-1.704 857	2.602 337	6.412 828	7
0	4	-4.519 910	2.263 955	7.444 429	8
0	6	-7.616 374	1.031 162	8.141 444	9
0	8	-10.856 049	-0.662 826	8.138 189	10
0	10	-14.186 766	-2.640 671	7.597 027	10
1	0	2.000 000	6.000 000	12.000 000	3
1	3	0.489 539	6.153 928	12.285 114	8
1	6	-2.675 243	5.535 499	12.865 402	9
1	9	-6.481 474	3.913 801	13.078 672	10
1	12	-10.628 924	1.630 021	12.620 576	11
1	15	-14.995 686	-1.093 056	11.558 712	12

the static dipole potential provided the dominant contribution to the binding, then it could be expected that for molecules with a single dipolar bond the values of r_0 would be approximately half the length of the molecular dipole (~ 1 au), with values significantly larger or smaller than this considered as unphysical. For molecules with several dipolar bonds (e.g., the formates and acetates) we expected a larger value of r_0 than in the case of a single dipole bond.

The results are shown in table 3. Clearly, all of the radii obtained are unphysically small, particularly for the most weakly polar molecules. The largest value, $r_0 = 0.5$ au, is for the most strongly polar molecule studied: 2-methylpropionitrile, but even this is less than a quarter of the $\text{C}\equiv\text{N}$ bond length.

It can be seen from table 3 that despite molecules of the same type (aldehyde, ketone, etc) having similar dipole moments, there can be significant variations in the binding energies. For example, consider the molecules acetaldehyde and butanal. Their dipole moments are very close (2.75 D and 2.72 D, respectively), and the dipole in both molecules is due to a $\text{C}=\text{O}$ bond. Yet there is a large difference in the binding energies: the binding energy for butanal (142 meV) is more than 1.5 times that for acetaldehyde (88 meV). Peculiarly, acetaldehyde is actually slightly more polar than butanal, yet has the lower binding energy. A similar situation also occurs with acetone and 2-butanone, and with ethyl formate and propyl formate. These observations cannot be explained by our model as it stands.

The fact that the values of r_0 obtained for all of the molecules studied are unphysically small implies that lepton correlations (in particular, due to polarization of the molecule by the positron) play an important role in enhancing the binding energy, even for strongly polar molecules. Going back to the example of acetaldehyde vs butanal, acetaldehyde has a polarizability of 4.6 \AA^3 , while the polarizability of butanal is a significantly greater value of 8.2 \AA^3 [37]. This explains the larger binding energy of the latter molecule. In the following two sections we investigate the effect of the molecular polarization on positron binding, and show that its

inclusion is critical for obtaining a correct physical picture of positron binding to polar molecules.

4. Perturbative correction due to molecular polarization

4.1. Core radii for perturbative inclusion of polarization

Since the dipole potential for $\mu > \mu_{\text{crit}}$ is sufficient to create a ‘zeroth-order’ bound state, we first estimate the effect of molecular polarization using perturbation theory. The values of the radius r_0 can then be chosen by fitting the total binding energy (i.e., due to the dipole force and polarization) to the experimental values, expecting that this should lead to more realistic values of r_0 .

The extra contribution to the positron potential energy (in the region $r > r_0$) due to molecular polarization can be approximated by the polarization potential

$$V_{\text{pol}}(\mathbf{r}) = -\frac{\alpha}{2r^4}, \quad (24)$$

where α is the molecular dipole polarizability. Using perturbation theory, the first-order correction to the original dipole binding energy (18), which we now label $\epsilon_b^{(0)}$, is

$$\epsilon_b^{(1)} = \int \frac{\alpha}{2r^4} |\psi_{011}(\mathbf{r})|^2 d^3\mathbf{r}, \quad (25)$$

where $\psi_{msn}(\mathbf{r}) = R_{msn}(r)\Phi_{ms}(\theta, \phi)$. Assuming that the radial and angular parts of the wave function are separately normalized to unity, this becomes

$$\epsilon_b^{(1)} = \frac{\alpha}{2} \int_{r_0}^{\infty} |R_{011}(r)|^2 r^{-2} dr. \quad (26)$$

For each of the molecules studied we made an initial estimate for the value of r_0 and adjusted it until the new binding energy $\epsilon_b = \epsilon_b^{(0)} + \epsilon_b^{(1)}$ was within 10% of the experimental value (with both $\epsilon_b^{(0)}$ and $\epsilon_b^{(1)}$ being functions of r_0). The results are shown in table 4. Polarizabilities are taken from the CRC Handbook [37], with the exceptions of propyl formate and cyclopentanone, for which the polarizabilities have been estimated by Danielson *et al* [7].

All of these new values of r_0 are significantly larger than the original values. The three nitriles are the most strongly polar molecules studied, and they now have very realistic values of r_0 . The dipole in these nitriles is due to the $\text{C}\equiv\text{N}$ bond. The length of this bond is 2.19 au [39], half of which is approximately 1.1 au. The values of r_0 are only slightly greater than this.

The ketones—acetone, 2-butanone and cyclopentanone—are the second most polar group. The polarity of these molecules is due to a $\text{C}=\text{O}$ bond, the length of which is 2.26 au [39] (half of this is 1.13 au). Their values of r_0 are not as close to this estimate as those for the nitriles. For the most polar molecule in the group, cyclopentanone, r_0 is within 19% of half the bond length. The values of r_0 for acetone and 2-butanone are, however, significantly smaller. The picture is similar for the aldehydes, which show $r_0 \sim 0.5$ au. The three

Table 4. Fitted values of r_0 with the inclusion of polarization via perturbation theory. Also shown are the corresponding values of $\epsilon_b^{(0)}$ and $\epsilon_b^{(1)}$, the expectation values of the potential energy due to the permanent dipole, and the predicted and experimental values of ϵ_b .

Molecule	μ (D)	α (\AA^3)	r_0 (au)	$\epsilon_b^{(0)}$ (meV)	$\epsilon_b^{(1)}$ (meV)	$ \langle V_d(\mathbf{r}) \rangle $ (meV)	ϵ_b (meV)	
							Pred.	Exp.
Aldehydes								
Acetaldehyde	2.75	4.6	0.60	3	80	38	83	88
Propanal	2.52	6.5	0.42	1	118	23	119	118
Butanal	2.72	8.2	0.58	2	140	35	142	142
Ketones								
Acetone	2.88	6.4	0.63	4	168	58	172	174
2-butanone	2.78	8.1	0.58	3	187	46	190	194
Cyclopentanone	3.30	9.0	0.92	10	220	98	230	230
Formates								
Methyl formate	1.77	5.1	0.004	$\sim 10^{-5}$	69	$\sim 10^{-2}$	69	65
Ethyl formate	1.98	6.9	0.066	$\sim 10^{-2}$	109	2	109	103
Propyl formate	1.89	8.8	0.0305	$\sim 10^{-3}$	126	$\sim 10^{-1}$	126	126
Acetates								
Methyl acetate	1.72	6.9	0.0006	$\sim 10^{-6}$	116	$\sim 10^{-4}$	116	122
Ethyl acetate	1.78	8.6	0.0048	$\sim 10^{-4}$	156	$\sim 10^{-2}$	156	160
Nitriles								
Acetonitrile	3.93	4.4	1.175	27	155	202	182	180
Propionitrile	4.05	6.3	1.24	31	218	218	249	245
2-methylpropionitrile	4.29	8.1	1.40	35	244	235	279	274
Methyl halides								
Methyl fluoride	1.86	2.4	0.042	$\sim 10^{-4}$	0.33	$\sim 10^{-2}$	0.33	0.3
Methyl chloride	1.90	4.4	0.026	$\sim 10^{-3}$	23	$\sim 10^{-1}$	23	25
Methyl bromide	1.82	5.6	0.0085	$\sim 10^{-3}$	42	$\sim 10^{-1}$	42	40

other groups (formates, acetates and methyl halides) have dipole moments $\mu \leq 2$ D, only slightly exceeding the critical dipole moment $\mu_{\text{crit}} = 1.625$ D. They all yield unphysically small values of r_0 .

The results suggest that our model, with the inclusion of polarizability via perturbation theory, is viable for molecules with dipole moments greater than about 3.5 D. It is of some concern that for all of the molecules studied, including those for which we have now found realistic values of r_0 , the first-order energy corrections $\epsilon_b^{(1)}$ are much larger than the zeroth-order energies $\epsilon_b^{(0)}$. However, one should compare the perturbative correction with the mean potential energy in the original dipole potential $\langle V_d \rangle$, not the eigenvalue (in which the negative potential energy and positive kinetic energy contributions noticeably cancel each other). Table 4 shows this information for all of the molecules studied. We see that for the most strongly polar molecules, e.g., the nitriles, $\langle V_d \rangle$ and $\epsilon_b^{(1)}$ are of similar magnitude. This indicates that the corresponding estimates of $\epsilon_b^{(1)}$ are reliable. On the other hand, for most of the other molecules, the magnitude of $\langle V_d \rangle$ is quite small compared to that of $\epsilon_b^{(1)}$. However, even in these cases the perturbation-theory estimate of the relative contribution of correlations (i.e., polarization) appears to be sound, at least qualitatively.

It is interesting to compare the results from table 4 with real quantum chemistry calculations of positron binding to polar species. The static dipole binding energy $\epsilon_b^{(0)}$ is then

analogous to the static, HF calculation of binding, while the total ϵ_b can be compared with the CI result, which includes correlations. In all cases the binding energy from the extensive CI calculations is at least an order of magnitude greater than the HF value. For example, for hydrogen cyanide (HCN, $\mu = 3$ D), the binding energies are 1.6 meV (HF) and 35 meV (CI) [16]; for formaldehyde (CH_2O , $\mu = 3$ D), 1.1 meV (HF) and 19 meV (CI) [15]; for nitrile molecules (CH_3CN , HCCCN , $\text{C}_2\text{H}_3\text{CN}$, $\text{C}_2\text{H}_5\text{CN}$ with $\mu = 4.1$ – 4.4 D), the HF binding energies are 6–18 meV, becoming 81–164 meV in the CI calculation² [19]. The data for aldehydes, ketones and nitriles in table 4 show similar large increases due to the effect of polarization. The model thus provides a useful estimate of the effect of correlations on the binding energy.

As mentioned in the introduction, analysis of the measured binding energies found the dependence of ϵ_b on α for molecules within the same chemical family (i.e., aldehydes, ketones, formates, acetates, nitriles) to be almost linear [7]. From (26) we can see that, for fixed μ and r_0 , $\epsilon_b^{(1)}$ scales linearly with α . Within each chemical family, the type of dipole is the same and so μ does not vary much. Thus, for the most part, the values of r_0 are fairly close to each other within each chemical family. This implies that considering the effect

² In all likelihood the above CI energies underestimate the true binding energy, because ‘it is difficult to describe the electron–positron correlation with the established methods of computational chemistry’ [40].

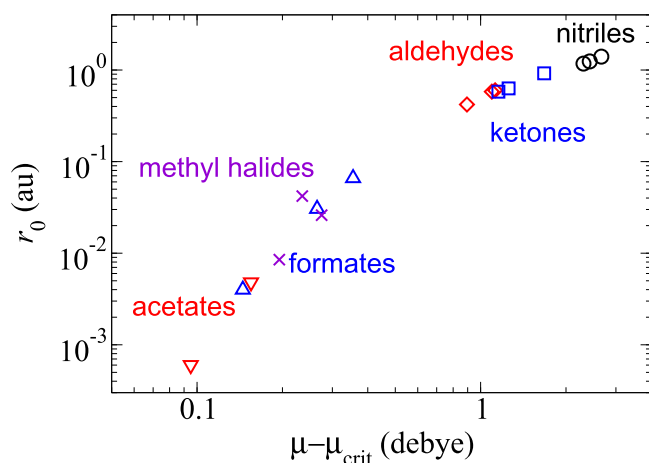


Figure 4. Correlation between the molecular dipole moment and core radius r_0 , obtained from the perturbative polarization calculation (see table 4) for nitriles (circles), ketones (squares), aldehydes (diamonds), formates (up triangles), acetates (down triangles), and methyl halides (crosses).

of polarization as the first-order energy correction might be quite realistic, even when α is large.

4.2. Dependence of the binding energy on polarizability for fixed μ and r_0

The new values of r_0 (those obtained after including the polarizability) correlate strongly with the dipole moment of the molecules (see figure 4). However, this correlation lacks an obvious physical basis, and predicting the binding energy for an arbitrary molecule given only the values of μ and α would be rather tenuous.

On the other hand, as was stated earlier, the dipole moment μ and core radius r_0 do not change vastly from molecule to molecule within each chemical family, for most of the families studied. To investigate the dependence of ϵ_b on α , we assigned to each family a fixed value of μ and r_0 . For five out of the six families, each with three molecules, we used the values of μ and r_0 for the molecule with the median value of μ . This molecule will hereafter be referred to as the *base molecule*. For the two acetates, we arbitrarily chose ethyl acetate as the base molecule.

For the base molecule we know $\epsilon_b^{(0)}$ and $\epsilon_b^{(1)}$. By setting α to the appropriate values for the other molecules in the family, we were able to find the corresponding $\epsilon_b^{(1)}$: they are just linear rescalings of (26), since μ and r_0 had not changed. With $\epsilon_b^{(0)}$ fixed by the values of μ and r_0 for the base molecule, we then had estimates of ϵ_b for every molecule in the family.

Table 5 compares the predicted and experimental values of the binding energy for the seventeen molecules studied. We also use this method to predict the binding energy of HCN, placing it in the aldehyde family (see below). The results for each family are also shown graphically in figure 5. The dashed lines on the graphs show linear fits of the measured binding energies, while the solids lines display the

linear dependence of the calculated binding energy on α , as described by equation (26).

For the aldehydes, the results are very good. In particular, note the similar slopes of the experimental and predicted dependences of the binding energy on α . The predicted binding energies of acetaldehyde and propanal agree with the experimental values to within 8% and 5% respectively.

For the ketones, the results are again pleasing. The predicted binding energies of 2-butanone and cyclopentanone agree with the experimental values to within 12% and 5% respectively.

The formates also yield good results. The predicted binding energies of methyl formate and ethyl formate agree with the experimental values to within 13% and 4% respectively. It is actually quite surprising that the predicted binding energies are as accurate as they are for this family, since r_0 for methyl formate is an order of magnitude smaller than the values for the rest of the family, and r_0 for ethyl formate is more than double the value for propyl formate.

The predicted binding energy for methyl acetate is excellent; it is within 3% of the experimental value. Again, this is fairly surprising, given that r_0 for methyl acetate is an order of magnitude smaller than the value for ethyl acetate. Note also that the α scaling holds well for both the formates and acetates in spite of the unphysically small values of r_0 .

Coming to the nitriles, we note the very encouraging results. The predicted binding energies of acetonitrile and 2-methylpropionitrile agree with the experimental values to within 2% and 14% respectively.

Finally, we note that for methyl halides the present model fails completely. The predicted binding energies for CH_3Cl and CH_3Br are only 2% of the measured values. At this point, we note that methyl halides are the smallest molecules examined. The lightest of them, methyl fluoride, also has the smallest moment of inertia, which means that molecular rotations neglected by the model have the largest effect on this molecule. This, combined with the smallest dipole polarizability, could be one of the reasons for the anomalously small binding energy (0.3 meV) of this molecule. Hence, when the ‘atypical’ CH_3F is chosen as the base molecule, the results for the other two molecules are poor. Another reason that sets methyl halides apart is that other molecules within each family consist of the same types of atoms. They are quite similar chemically and have similar ionization potentials (typically, not varying by more than 0.5 eV within each family [37]). On the other hand, the three methyl halide molecules contain different atoms (F, Cl or Br), and their ionization potentials vary considerably more: 12.47, 11.22 and 10.54 eV for CH_3F , CH_3Cl and CH_3Br respectively [37]. This means that the additional attraction due to virtual positronium formation, which is not accounted for by the dipole polarizability (see, e.g., [41]), grows along this sequence. Since this additional attraction is not present in our model, we obtain very poor predictions of binding energies. At the same time, the dipole moment, even though not much greater than μ_{crit} , plays a crucial role for binding by these molecules. Had these been nonpolar, atom-like species, then, based on the their ionization potentials and dipole

Table 5. The predicted values of ϵ_b found by using fixed values of μ and r_0 for each chemical family, compared with the experimental values. Hydrogen cyanide is included with the aldehydes as it has a similar dipole moment; the value of ϵ_b for hydrogen cyanide obtained using the diffusion Monte Carlo (DMC) method [17] is also given. The base molecule for each family is indicated by '(base)' after its name.

Molecule	μ (D)	r_0 (au)	α (\AA^3)	ϵ_b (meV)	
				Pred.	Exp./DMC
Aldehydes					
Butanal (base)	2.72	0.58	8.2	142	142
Acetaldehyde	"	"	4.6	81	88
Propanal	"	"	6.5	113	118
(Hydrogen cyanide)	"	"	2.5	45	38
Ketones					
Acetone (base)	2.88	0.63	6.4	172	174
2-butanone	"	"	8.1	216	194
Cyclopentanone	"	"	9.0	240	230
Formates					
Propyl formate (base)	1.89	0.0305	8.8	126	126
Methyl formate	"	"	5.1	73	65
Ethyl formate	"	"	6.9	99	103
Acetates					
Ethyl acetate (base)	1.78	0.0048	8.6	156	160
Methyl acetate	"	"	6.9	125	122
Nitriles					
Propionitrile (base)	4.05	1.24	6.3	249	245
Acetonitrile	"	"	4.4	183	180
2-methylpropionitrile	"	"	8.1	311	274
Methyl halides					
Methyl fluoride (base)	1.86	0.042	2.4	0.33	0.3
Methyl chloride	"	"	4.4	0.61	25
Methyl bromide	"	"	5.6	0.78	40

polarizabilities, they would not have had bound states at all (see [42] for the conditions of binding by atoms).

Overall, the perturbative treatment of polarization has been surprisingly good for the five families of organic molecules. The maximum error in any of the predicted binding energies is 14%, even though two of the five families exhibit small absolute values of r_0 with significant relative differences in the values of r_0 . The model also lends support to the empirical linear relationship (2) between the binding energy and the dipole polarizability, even though the values of r_0 for most molecules are unphysically small.

In addition, it allows one to predict the binding energy for any molecule with a dipole moment that is comparable to those in one of the chemical families studied, by placing it in that group and rescaling $\epsilon_b^{(1)}$ using the appropriate polarizability.

As an example, consider hydrogen cyanide (HCN), which is a linear, triatomic molecule with a dipole moment of 2.98 D and a polarizability of 2.5 \AA^3 [37]. Due to its toxicity, the binding energy for hydrogen cyanide has not been measured experimentally. Nevertheless, there already exist theoretical calculations of this energy using a variety of methods, such as CI and diffusion Monte Carlo (DMC) [16, 17]. We estimated the binding energy by placing hydrogen cyanide among the aldehydes, since they have similar dipole moments. The resulting prediction of the binding energy (45 meV) is within 18% of the DMC value of 38 meV [17]

(see table 5 and figure 5). Note that the ketones actually have more similar dipole moments to hydrogen cyanide than the aldehydes. Placing HCN in the ketone family led to a predicted binding energy of 70 meV, which is a factor of two greater than the DMC result of [17]. This large value is likely an overestimate, in spite of the fact that quantum chemistry calculations tend to give lower bounds for the positron binding energies [19, 20]. Experimental data for ketones shows significant deviations from linearity (see figure 5), which makes the ketone-based prediction for HCN less reliable.

5. Non-perturbative treatment of molecular polarization

5.1. Models of polarization potential and core radii

Although the perturbative inclusion of polarization described in section 4 generates reasonably accurate predictions of binding energies for organic molecules, the effective core radii r_0 are too small for most molecules to be physically meaningful. In addition, the first-order polarization energy correction for most molecules is too large to justify the use of perturbation theory. To overcome this limitation, in this section we include the polarization potential in a full, non-perturbative manner. As we will see, this leads to new

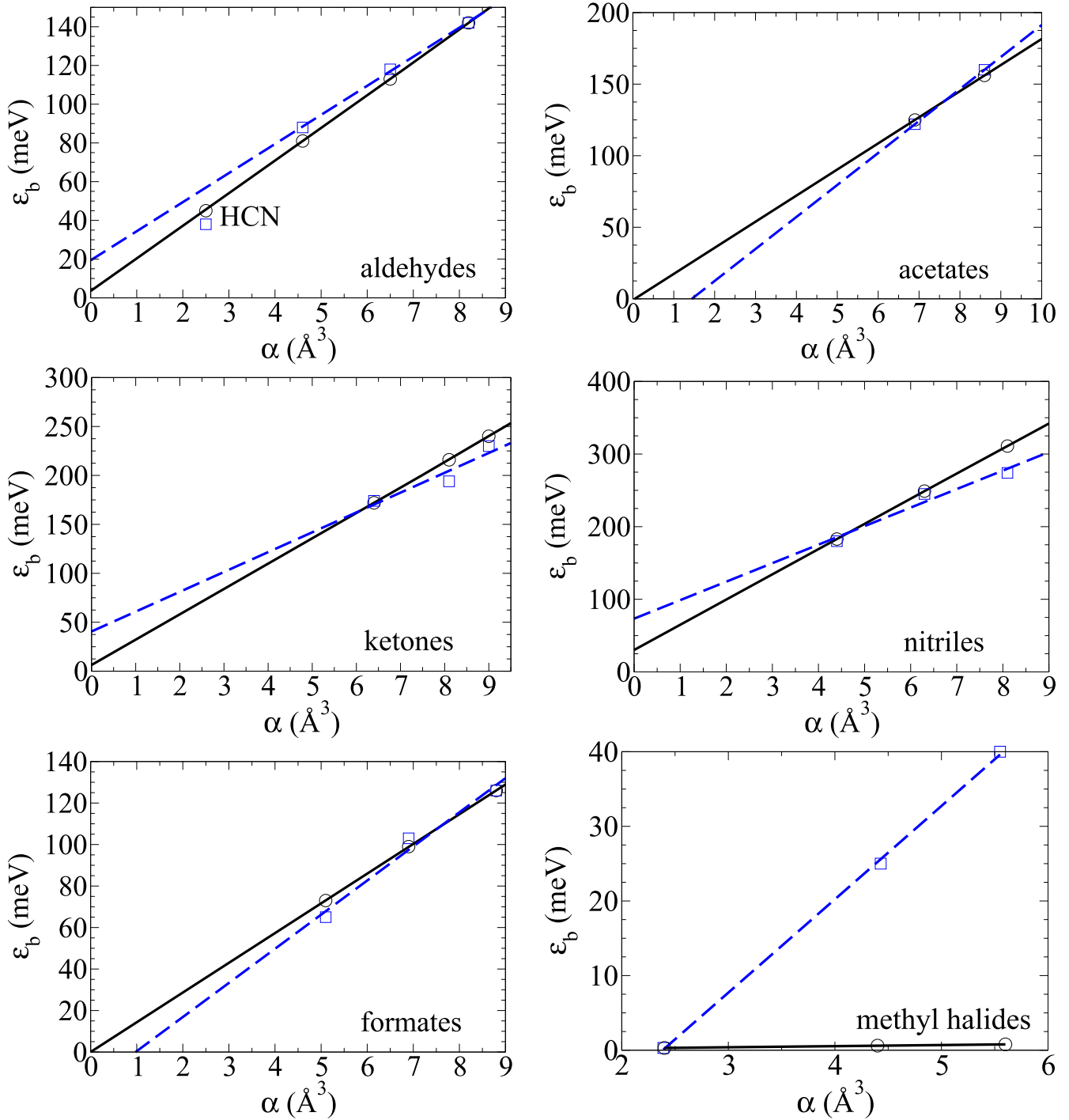


Figure 5. Predicted and experimental/DMC values of ϵ_b as functions of the dipole polarizability. The black circles and black, solid line are the predicted values of ϵ_b . The blue squares are the experimental/DMC values of ϵ_b , with the blue, dashed line a linear regressive fit.

physical insights and finally gives good physical values of r_0 for all molecules.

When the polarization potential (24) is added to the Schrödinger equation (4), the angular equation (5b) remains unchanged, and we have the radial equation

$$-\frac{1}{2} \frac{d^2 P_{msn}}{dr^2} + \left[\frac{\lambda_{ms}}{2r^2} - \frac{\alpha}{2r^4} g(r) \right] P_{msn}(r) = E_{msn} P_{msn}(r), \quad (27)$$

for the function $P_{msn}(r) \equiv rR_{msn}(r)$. Here we have also introduced the polarization cut-off function $g(r)$, which tends to unity at large r and moderates the unbounded, unphysical growth of the $-\alpha/2r^4$ term at small distances (see, e.g., [3]; also see below).

At large r , the polarization potential is negligible in comparison with the $1/r^2$ dipole potential. Thus, at some sufficiently large value of $r = r_{\max}$ the radial wave function is

given by equation (14), which gives the boundary conditions

$$P_{msn}(r_{\max}) = \tilde{A}_{msn} \sqrt{r_{\max}} K_{i\beta_{ms}}(\kappa_{msn} r_{\max}), \quad (28a)$$

$$\left. \frac{dP_{msn}(r)}{dr} \right|_{r=r_{\max}} = \tilde{A}_{msn} \frac{d}{dr} \left[\sqrt{r} K_{i\beta_{ms}}(\kappa_{msn} r) \right] \Big|_{r=r_{\max}}, \quad (28b)$$

where \tilde{A}_{msn} is an arbitrary constant. A value of $r_{\max} = 30$ au has been used throughout. Solving equation (27) numerically in the interval $0 < r \leq r_{\max}$ with $m = 0$, $s = n = 1$, $E_{011} = -\epsilon_b$, and $\tilde{A}_{011} = r_{\max}^{-1/2}$ yields a real function $P_{011}(r)$ with infinitely many roots accumulating at $r = 0$. The largest of these roots is the value of r_0 .

We initially considered $g(r) = 1$, as in section 4. This led to values of r_0 in the range 1.55–2.32 au across the six families of molecules, which are much greater than their perturbative counterparts, and probably too large to be considered physical. This is due to the polarization potential (24) blowing up and causing a rapid variation of the radial wave function at small r , while in reality the polarization is a long-range effect. For the same reason, the binding energy was found to be extremely sensitive to the value of r_0 , making it very difficult to use the model in a predictive way.

Consequently, we considered several cut-off functions, viz.

$$g_1(r) = 1 - \exp(-r^6/r_c^6), \quad (29a)$$

$$g_2(r) = \frac{r^4}{(r + r_c)^4}, \quad (29b)$$

$$g_3(r) = \frac{r^4}{(r^2 + r_c^2)^2}, \quad (29c)$$

where r_c is a cut-off radius for the polarization. The function $g_1(r)$ provides a very rapid cut-off, and is commonly used to model polarization potentials in atoms [3]. The functions $g_2(r)$ and $g_3(r)$ vary much more slowly. They can effectively account for the fact that the ‘centre’ of the polarization potential is usually off-set with respect to the location of the molecular dipole. The dipole moment is usually associated with one of the terminal bonds, which is near one of the ‘ends’ of the molecule rather than in the middle. Initially we worked with fixed values of r_c across the entire set of molecules, and though this reduced the values of r_0 from those of the ‘hard’ potential ($g(r) = 1$), and also reduced the sensitivity of the binding energy to r_0 , it did not significantly reduce the large spread in r_0 within or between families. This led us to consider using a polarizability-dependent cut-off radius.

The polarizability of organic molecules is generally proportional to the number of atoms or number of bonds in the molecule. This idea is the physical basis behind various additivity methods for the calculation of molecular polarizabilities [43]. In this spirit, the polarization potential at large distances is the sum of terms $-\alpha_i/2r_i^4$ due to the contribution of individual atoms or bonds i , with the distance r_i measured accordingly. In the spherically-averaged form (24), the distance r must be measured from the ‘centre of polarization’ rather than the centre of the molecular dipole. As a result, at small r

Table 6. Values of r_0 when a soft polarization potential with the cut-off function $g_3(r)$ is included non-perturbatively and r_c given by equation (4) with $\nu = \frac{1}{2}$. The parameter C is given in units of $a_0 \text{ \AA}^{-3/2}$, where a_0 is the Bohr radius.

Molecule	μ (D)	α (\AA^3)	ϵ_b (meV)	r_0 (au)
Aldehydes ($C = 1.08$)				
Acetaldehyde	2.75	4.6	88	1.17
Propanal	2.52	6.5	118	1.09
Butanal	2.72	8.2	142	1.16
Ketones ($C = 0.98$)				
Acetone	2.88	6.4	174	1.24
2-butanone	2.78	8.1	194	1.24
Cyclopentanone	3.30	9.0	230	1.37
Formates ($C = 1.06$)				
Methyl formate	1.77	5.1	65	0.94
Ethyl formate	1.98	6.9	103	0.98
Propyl formate	1.89	8.8	126	0.94
Acetates ($C = 0.96$)				
Methyl acetate	1.72	6.9	122	1.05
Ethyl acetate	1.78	8.6	160	1.05
Nitriles ($C = 1.12$)				
Acetonitrile	3.93	4.4	180	1.34
Propionitrile	4.05	6.3	245	1.34
2-methylpropionitrile	4.29	8.1	274	1.43
Methyl halides ($C = 0.95$)				
Methyl fluoride	1.86	2.4	0.3	1.22
Methyl chloride	1.90	4.4	25	1.24
Methyl bromide	1.82	5.6	40	1.24

the singular form $-\alpha/2r^4$ must be replaced by a constant $-\alpha/2r_c^4$, as described by the cut-off functions $g_2(r)$ and $g_3(r)$. Here r_c is the effective radius of the molecule. It is physical to link it to the polarizability α by, e.g.

$$r_c = C\alpha^\nu, \quad (4)$$

with C being an adjustable parameter. The polarizability α has dimensions of volume (i.e., length cubed), so the choice $\nu = \frac{1}{3}$ would be sensible for three-dimensional, approximately spherical molecules, while $\nu = \frac{1}{2}$ would be better for approximately planar molecules. Experimentation showed that $\nu = \frac{1}{2}$ works best for our set of molecules, with C being chosen separately for each family to minimize the range of values of r_0 within the family.

Table 6 shows the final values of r_0 obtained for the molecules, with $r_c = C\alpha^{1/2}$. As expected, the cut-off functions $g_2(r)$ and $g_3(r)$ gave the most physically meaningful results, with neither being significantly better or worse than the other. Here we present the results obtained using $g_3(r)$. Figure 6 compares the radial function $P_{011}(r)$ for acetonitrile, with and without the non-perturbative inclusion of the polarization potential. It is clear from the figure that the wave function does not change much for $r > 5$ au. However, at smaller distances the addition of the polarization potential causes a more rapid variation of the wave function, leading to a greater core radius r_0 .

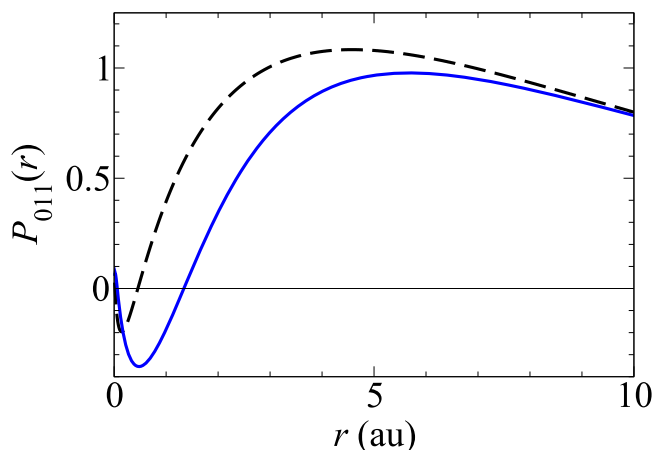


Figure 6. Radial wave functions for acetonitrile. The dashed black curve is without the inclusion of polarization; the solid blue curve is with the polarization included non-perturbatively, using the cut-off function $g_3(r)$.

As seen from table 6, all of the radii are now ~ 1 au and hence look physically meaningful. They also remain approximately constant within each chemical family. The maximum range of r_0 within any family is 0.13 au (for the ketones), and the range across all the molecules is 0.49 au. The values of C are also quite consistent, ranging from 0.95 to $1.12 a_0 \text{ \AA}^{-3/2}$. As before, the largest radii are obtained for the most strongly polar molecules (the nitriles) and the smallest radii are obtained for the most weakly polar molecules (the formates and acetates).

5.2. Dependence of the binding energy on polarizability for fixed μ and r_0

We can now again investigate the dependence of the binding energy on the molecular polarizability, by fixing μ and r_0 within each family and varying α . In these calculations we choose the same base molecule within each family as in section 4.2. The binding energy which enters in equation (27) is then adjusted for each molecule in the family until the core radius r_0 of the base molecule is obtained. Note that the polarization potential is now included non-perturbatively, hence, there is no reason to expect that ϵ_b depends linearly on α . The resulting binding energies are shown in table 7 and figure 7.

There is generally very close agreement between the model predictions and the experimental data; for every molecule except methyl formate and methyl acetate, the relative difference of the predicted binding energy from the experimental value is smaller than it was using the perturbative method. Particularly noteworthy is 2-methylpropionitrile, for which the predicted binding energy coincides exactly with the experimental value. The error for methyl formate has increased from 13% to 18%, and for methyl acetate it has increased from 3% to 4%.

From figure 7 it is apparent that when the polarization potential is included non-perturbatively, the dependence of ϵ_b on α is indeed nonlinear. For all families except the methyl

halides, ϵ_b increases convexly with α for $\alpha \lesssim 4 \text{ \AA}^3$; for $\alpha \gtrsim 4 \text{ \AA}^3$ the growth becomes concave. The molecules studied all lie in the concave region, and the growth for them could be reasonably well approximated by a straight line. The prediction curve for the methyl halides is different but particularly remarkable, as the description of this molecular family was extremely poor in the perturbative treatment. Here the molecules lie in the convex region (which spans a larger range of polarizabilities than for the other families), and the dependence of ϵ_b on α is markedly nonlinear. However, close agreement is observed with the measured binding energies for CH_3Cl and CH_3Br .

Table 7 and figure 7 also show our estimate of the binding energy for HCN. As seen from the graph, the experimental value lies very close to the prediction curve for the aldehydes data, which provides support that the dependence of ϵ_b on α is not truly linear. The value obtained (32 meV) is within 16% of the DMC calculation (38 meV) [17], which is slightly closer than our perturbative estimate. Interestingly, if we now place HCN in the ketones family, its estimated binding energy becomes 40 meV, in very close accord with the DMC value. This is further evidence that a nonperturbative treatment of molecular polarization gives overall much more consistent results. Note that smaller values of C have been obtained for the molecules in which the main dipole bond is located closer to the centre of the molecule (as in acetates and ketones with $C = 0.96$ and 0.98 , respectively). Larger values of C are obtained for the molecules in which the dipole bond is at the end, as in formates, aldehydes and nitriles ($C = 1.06$, 1.08 and 1.12 , respectively). This behaviour is related to the effect of the distance between the dipole bond and the centre of polarizability, which is greater for similar-sized molecule in the latter families. This results in greater binding energies for the acetate and ketone molecules relative to their formate and aldehyde counterparts with similar μ and α , e.g., methyl acetate (122 meV) vs ethyl formate (103 meV), or acetone (174 meV) vs propanal (118 meV).

6. Concluding remarks

Here we provided a simple model for positron binding to polar molecules, which captures the essential physics of this system.

Modelling the molecule as a sphere of radius r_0 with a static point dipole of dipole moment μ at the centre and using experimental data on binding energies required unphysically small values of r_0 , even for the most strongly polar molecules. This indicated that the binding energies are greatly enhanced by some factor other than the molecule's permanent dipole moment, i.e., electron-positron correlations.

Including the effect of correlations perturbatively through the polarization potential did confirm this expectation. It showed that even for the strongly polar molecules, the effect of correlations increased the binding energy by an order of magnitude compared to the static-dipole calculation. The observed increase matched the difference between the CI and

Table 7. The predicted values of ϵ_b found by using fixed values of μ and r_0 for each chemical family with the polarization included non-perturbatively, compared with the experimental values. Hydrogen cyanide is included with the aldehydes as it has a similar dipole moment; the value of ϵ_b for hydrogen cyanide obtained using the diffusion Monte Carlo method [17] is also given. The base molecule for each family is indicated by '(base)' after its name.

Molecule	μ (D)	r_0 (au)	α (\AA^3)	ϵ_b (meV)	
				Pred.	Exp./DMC
Aldehydes					
Butanal (base)	2.72	1.16	8.2	142	142
Acetaldehyde	"	"	4.6	86	88
Propanal	"	"	6.5	122	118
[Hydrogen cyanide]	"	"	2.5	32	38
Ketones					
Acetone (base)	2.88	1.24	6.4	174	174
2-butanone	"	"	8.1	210	194
Cyclopentanone	"	"	9.0	225	230
Formates					
Propyl formate (base)	1.89	0.94	8.8	126	126
Methyl formate	"	"	5.1	77	65
Ethyl formate	"	"	6.9	106	103
Acetates					
Ethyl acetate (base)	1.78	1.05	8.6	160	160
Methyl acetate	"	"	6.9	127	122
Nitriles					
Propionitrile (base)	4.05	1.34	6.3	245	245
Acetonitrile	"	"	4.4	200	180
2-methylpropionitrile	"	"	8.1	274	274
Methyl halides					
Methyl fluoride (base)	1.86	1.24	2.4	0.3	0.3
Methyl chloride	"	"	4.4	20	25
Methyl bromide	"	"	5.6	42	40

HF binding energies obtained in state-of-the-art quantum chemistry calculations.

Including the polarization potential as a perturbation of the original Hamiltonian also yielded larger, more physical values of r_0 for all of the molecules studied, but for most molecules they were still too small to be interpreted directly. This was partly due to the fact that the true static potential for the positron near the molecule is less repulsive than the hard wall of our model. Reduced values of r_0 may also account for some of the short-range correlation effects, such as virtual positronium formation. Sensible values of r_0 were, however, obtained for the nitriles, the most strongly polar of all the molecules studied. In spite of the fact that most of the molecules had unphysical values of r_0 , it was found that taking the value of μ and r_0 for the molecule in each chemical family with the median dipole moment and varying the polarizability to match the other molecules in the family, gave reliable predictions of the binding energies for those molecules (with the exception of the methyl halides). The perturbative treatment was also in line with the observation made by experimentalists, that the dependence of the binding energy on the polarizability of the molecule is apparently almost linear [7]. Of course, a general increase in the binding energy with the polarizability could be expected, but there was no explanation for the linear dependence. According to our model, this feature indicates that the perturbation theory is at

least qualitatively correct, even though the first-order energy corrections are generally greater than the original (dipole) eigenenergies. The results of this treatment for the methyl halides, however, were very poor in comparison with the other families, and we attributed this to the fact that the binding by the base molecule CH_3F is likely affected by rotations, and that the three methyl halide molecules had a significantly larger range of ionization potentials than the other families. The latter could indicate a significant change in the contribution of virtual positronium formation across the members of this family, which is not accounted for in our model.

A test of the model was to use it to predict the binding energy for hydrogen cyanide, which has not been measured experimentally. Our estimate agreed with a previous calculation using the DMC method to within 20%, which provides evidence that our model has good predictive power and could be useful for estimating the binding energies that have never been measured in experiment, provided that the binding energy for a molecule with a similar value of μ is known.

The most glaring limitation of the model as it stood was that it could not predict binding energies using only the dipole moment and polarizability of a molecule. To perform a calculation one needed a value of r_0 , and unless binding energies for molecules with similar values of μ were known, one could not easily choose a suitable value for r_0 . In fact, we found that

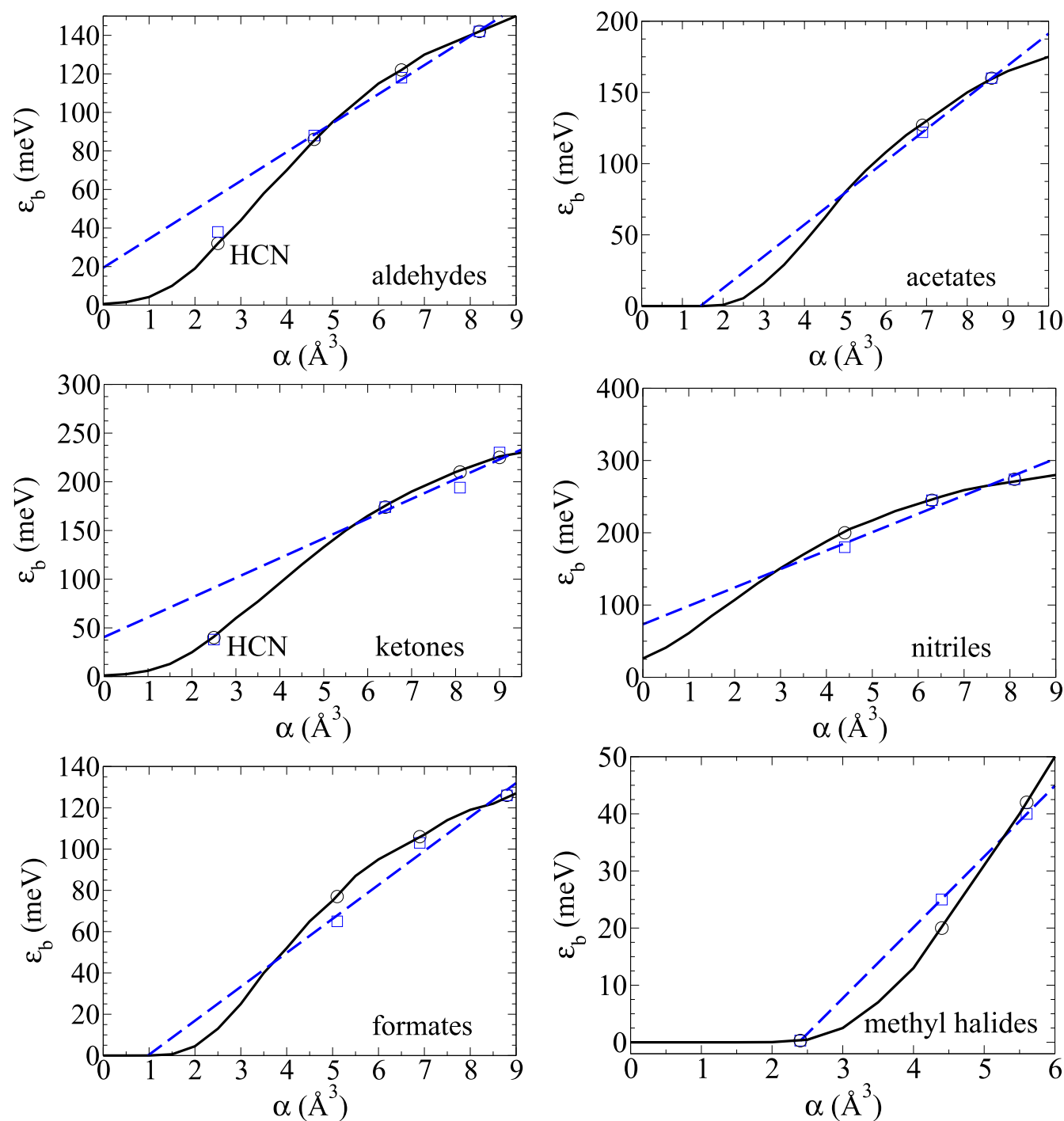


Figure 7. Predicted and experimental/DMC values of ϵ_b as functions of the dipole polarizability, obtained using the non-perturbative inclusion of the polarization potential. The black circles are the predicted values of ϵ_b , with the black, solid curve showing the calculated dependence of ϵ_b on α for each family. The blue squares are the experimental/DMC values of ϵ_b , with the blue, dashed line a linear regressive fit.

for most of the chemical families we considered the values of r_0 had no immediate physical relevance, and for the most weakly polar families (i.e., formates and acetates) there were significant variations in the values of r_0 despite the similar values of μ .

In a bid to attain physically meaningful values of r_0 for all of the molecules, we proceeded to include the effects of polarization in a non-perturbative way. We experimented by

solving the radial Schrödinger equation numerically using several model polarization potentials, and found that the best results were obtained using a polarization potential of the form $-\alpha/2(r^2 + r_c^2)^2$, with the cut-off radius $r_c = C\alpha^{1/2}$ (C being a constant). The parameter C was chosen separately for each chemical family so as to minimize the spread of r_0 within each family. Physically meaningful values of r_0 (in the range 0.94–1.43 au) were then obtained for all molecules. By

choosing the values of C carefully, the spread of values of r_0 within in each family was made relatively small, though there was inevitably still a larger range of 0.49 au across the entire set of molecules. The most strongly (weakly) polar molecules still possessed the largest (smallest) values of r_0 . Again fixing μ and r_0 for each family and varying only the polarizability led to excellent predictions of ϵ_b ; the predictions were generally more accurate than their perturbative counterparts, with particularly large improvement for the methyl halides. We observed that the true dependence of ϵ_b on α is actually nonlinear. The prediction for HCN was also slightly better than its perturbative counterpart, and supported our observation of nonlinear growth of ϵ_b with α .

In summary, our model can be used effectively to predict positron–molecule binding energies based on the molecular dipole moment and dipole polarizability, particularly when polarization is included in a non-perturbative way. It provides a clear picture of the system, thereby complementing the current computational effort towards rigorous theory of positron–molecule binding.

Acknowledgments

The authors are grateful to I I Fabrikant for useful discussions and suggestions.

References

- [1] Tuomisto F and Makkonen I 2013 *Rev. Mod. Phys.* **85** 1583
- [2] Wahl R L 2002 *Principles and Practice of Positron Emission Tomography* (Philadelphia: Lippincott Williams & Wilkins)
- [3] Mitroy J, Bromley M W J and Ryzhikh G G 2002 *J. Phys. B: At. Mol. Opt. Phys.* **35** R81
- [4] Gribakin G F, Young J A and Surko C M 2010 *Rev. Mod. Phys.* **82** 2557
- [5] Gilbert S J, Barnes L D, Sullivan J P and Surko C M 2002 *Phys. Rev. Lett.* **88** 043201
- [6] Danielson J R, Gosselin J J and Surko C M 2010 *Phys. Rev. Lett.* **104** 233201
- [7] Danielson J R, Jones A C L, Gosselin J J, Natisin M R and Surko C M 2012 *Phys. Rev. A* **85** 022709
- [8] Danielson J R, Young J A and Surko C M 2009 *J. Phys. B* **42** 235203
- [9] Gribakin G F and Lee C M R 2006 *Nucl. Instrum. Methods Phys. Res. B* **247** 31
- [10] Gribakin G F and Lee C M R 2009 *Eur. Phys. J. D* **51** 51
- [11] Mitroy J and Zhang J Y 2011 *Phys. Rev. A* **83** 064701
- [12] Koyanagi K, Takeda Y, Oyamada T, Kita Y and Tachikawa M 2013 *Phys. Chem. Chem. Phys.* **15** 16208
- [13] Koyanagi K, Kita Y and Tachikawa M 2013 *Int. J. Quantum Chem.* **113** 382
- [14] Tachikawa M, Buenker R J and Kimura M 2003 *J. Chem. Phys.* **119** 5005
- [15] Strasburger K 2004 *Struct. Chem.* **15** 415
- [16] Chojnacki H and Strasburger K 2006 *Mol. Phys.* **104** 2273
- [17] Kita Y, Maezono R, Needs R J, Tachikawa M and Towler M 2009 *J. Chem. Phys.* **131** 134310
- [18] Romero J, Charry J A, Flores-Moreno R, Varella M T d N and Reyes A 2014 *J. Chem. Phys.* **141** 114103
- [19] Tachikawa M, Kita Y and Buenker R J 2011 *Phys. Chem. Chem. Phys.* **13** 2701
- [20] Tachikawa M, Kita Y and Buenker R J 2012 *New J. Phys.* **14** 035004
- [21] Tachikawa M 2014 *J. Phys. Conf. Ser.* **488** 012053
- [22] Amaral P H R and Mohallem J R 2012 *Phys. Rev. A* **86** 042708
- [23] Ostrovsky V N 2001 *Found. Chem.* **3** 145
- [24] Ostrovsky V N 2003 *Ann. N. Y. Acad. Sci.* **988** 182
- [25] Khersonskii V K, Moskalev A N and Varshalovich D A 1988 *Quantum Theory of Angular Momentum* (Singapore: World Scientific Publishing)
- [26] Landau L D and Lifshitz E M 1965 *Quantum Mechanics: Non-Relativistic Theory* 2nd edn (Oxford: Pergamon)
- [27] Fermi E and Teller E 1947 *Phys. Rev.* **72** 399
- [28] Crawford O H 1967 *Proc. Phys. Soc.* **91** 279
- [29] Garrett W R 1971 *Phys. Rev. A* **3** 961
- [30] Crawford O H and Garrett W R 1977 *J. Chem. Phys.* **66** 4968
- [31] Abramowitz M and Stegun I A (ed) 1964 *Handbook of Mathematical Functions: with Formulas, Graphs, and Mathematical Tables* (New York: Dover)
- [32] Watson G N 1922 *A Treatise on the Theory of Bessel Functions* (Cambridge: Cambridge University Press)
- [33] Ferreira E M and Sesma J 2006 *J. Comp. Appl. Math.* **211** 223
- [34] Abramov D and Komarov I 1972 *Theor. Math. Phys.* **13** 1090
- [35] Fabrikant I I 1983 *J. Phys. B: At. Mol. Opt. Phys.* **16** 1253
- [36] Young J A and Surko C M 2008 *Phys. Rev. A* **78** 032702
- [37] Lide D R (ed) 2008–2009 *CRC Handbook of Chemistry and Physics* 89th edn (Boca Raton, FL: CRC Press)
- [38] Gribakin G F and Lee C M R 2006 *Phys. Rev. Lett.* **97** 193201
- [39] NIST computational chemistry comparison and benchmark database (<http://cccbdb.nist.gov>)
- [40] Wolczyr M M, Strasburger K and Chojnacki H 2013 *Mol. Phys.* **111** 345
- [41] Dzuba V A, Flambaum V V, Gribakin G F and King W A 1995 *Phys. Rev. A* **52** 4541
- [42] Dzuba V A, Flambaum V V and Gribakin G F 2010 *Phys. Rev. Lett.* **105** 203401
- [43] Miller K J 1990 *J. Am. Chem. Soc.* **112** 8533